Morphological and opto-electrical properties of solution deposited Platinum counter electrode for low cost dye sensitized solar cells

Gopala Krishna.V.V.Thalluri,*[a] Marc Décultot,[b] Catherine Henrist*[ac] Jennifer Dewalque,[a] Pierre Colson,[a] Serge Habraken,[b] Donato Spoltore,[d] Jean Manca,[de] and Rudi Cloots*[ac]

[a]. Group of Research in Energy and ENvironnement from MATerials(GREEnMat), University of Liège,Chemistry Institute B6, Allée de la Chimie 3, Liège, 4000 (Belgium)
Fax:+3243663413;Tel:+3243663436
E-mail: vvgk.thalluri@ulg.ac.be, r.cloots@ulg.ac.be, catherine.henrist@ulg.ac.be

[b].HoloLab, University of Liège, Physics Department, Liège, 4000 (Belgium)

[c].Center for Applied Technology in Microscopy (CATµ), University of Liège,Chemistry Institute B6, Allée de la Chimie 3, Liège, 4000 (Belgium)

[d].Institute for Materials Research (IMO), Hasselt University, Wetenschapspark 1,Diepenbeek, 3590 (Belgium)

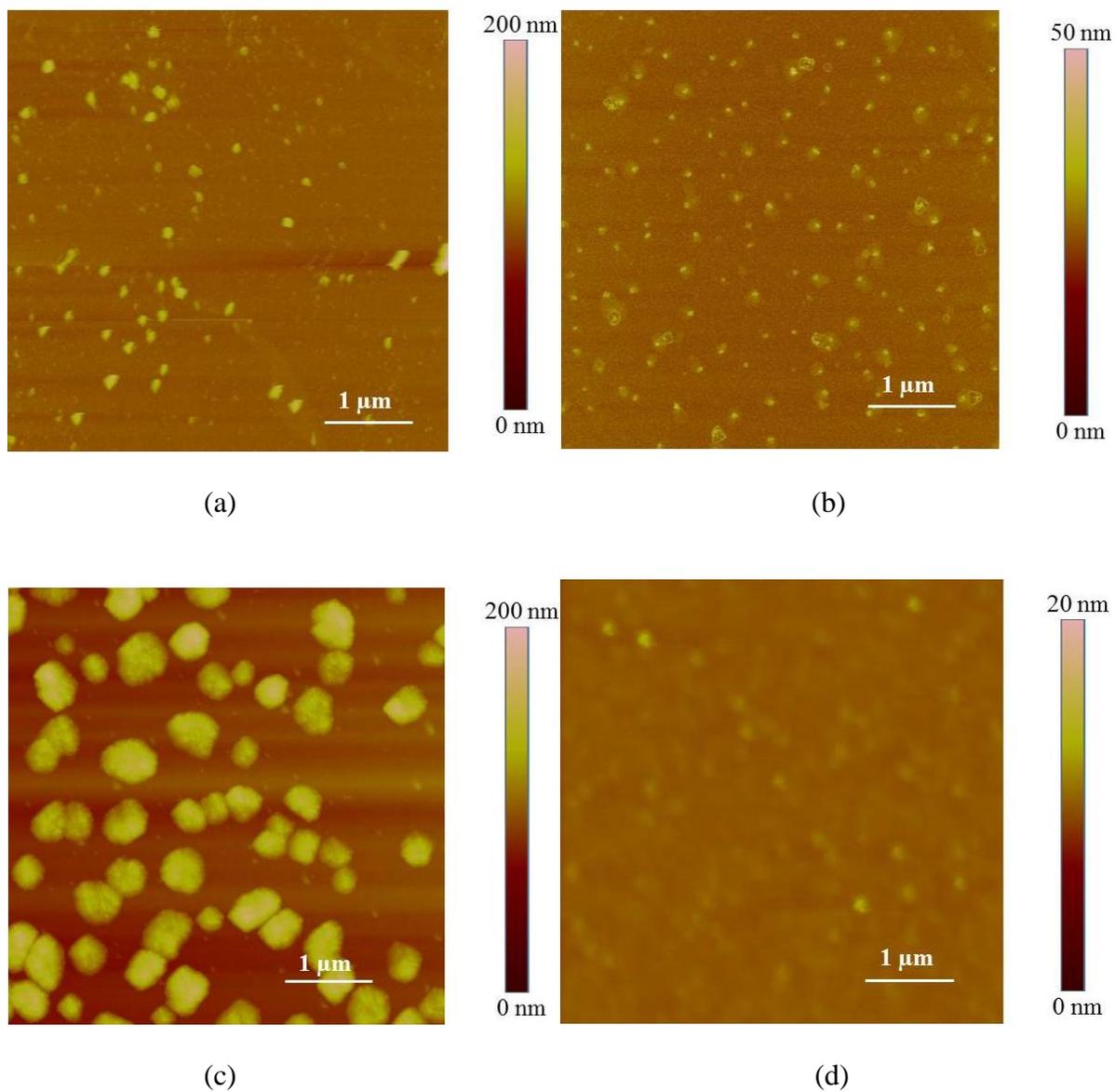*[e].IMEC-IMOMEC, vzw, Wetenschapspark 1,Diepenbeek, 3590 (Belgium)*

(a)

(b)

(c)

(d)

Fig S1. Atomic force microscope (AFM) measurements on the Pt-layers by various deposition techniques above Si substrates (a) spray-coated, (b) dip-coated, (c) brushed and (d) sputtered.
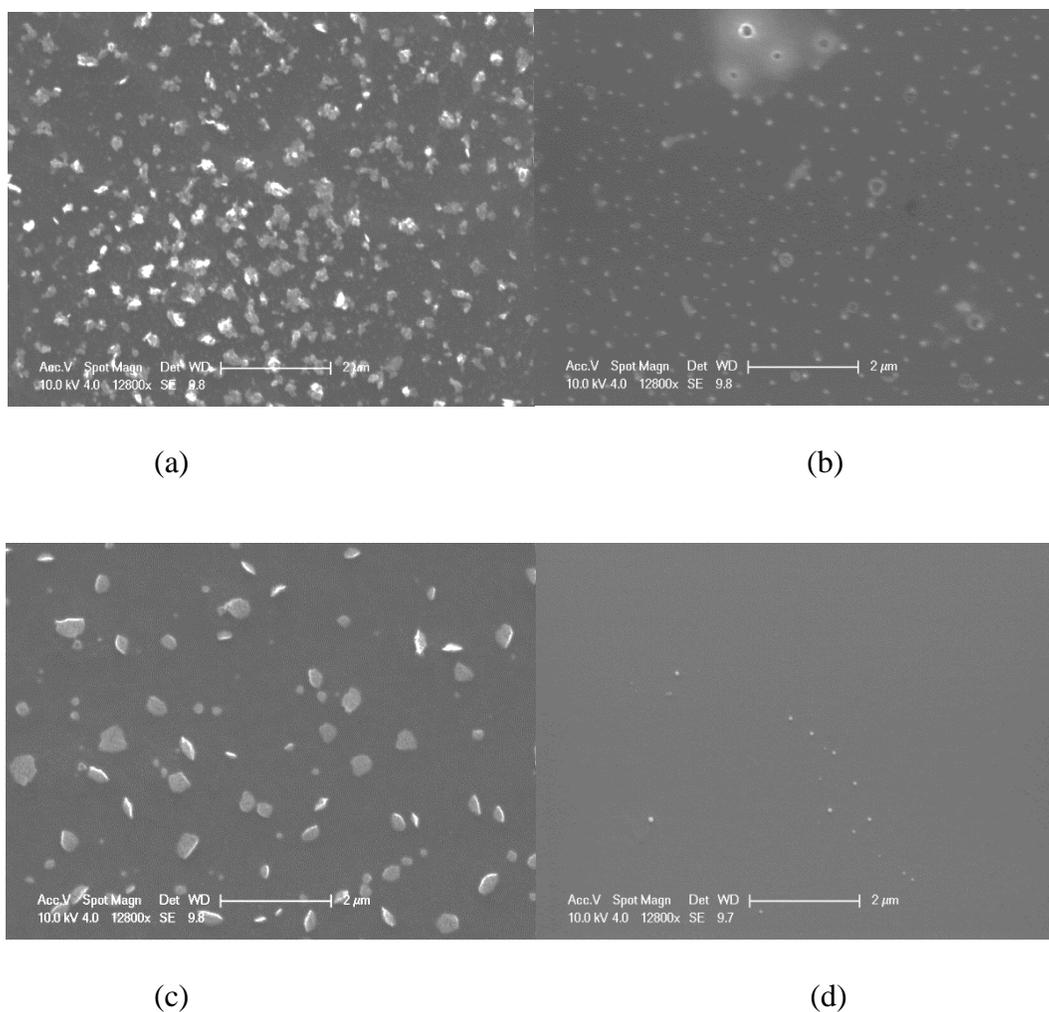
(a)

(b)

(c)

(d)

Fig S2. Scanning electron microscopy (SEM) measurements on the Pt-layers by various deposition techniques above Si substrates (a) spray-coated, (b) dip-coated, (c) brushed and (d) sputtered.

The SEM characterization (Fig S3) for the brushed Pt-layer with larger nanoclusters and each nanocluster were again constructed as two-dimensionally porous oriented template structure.
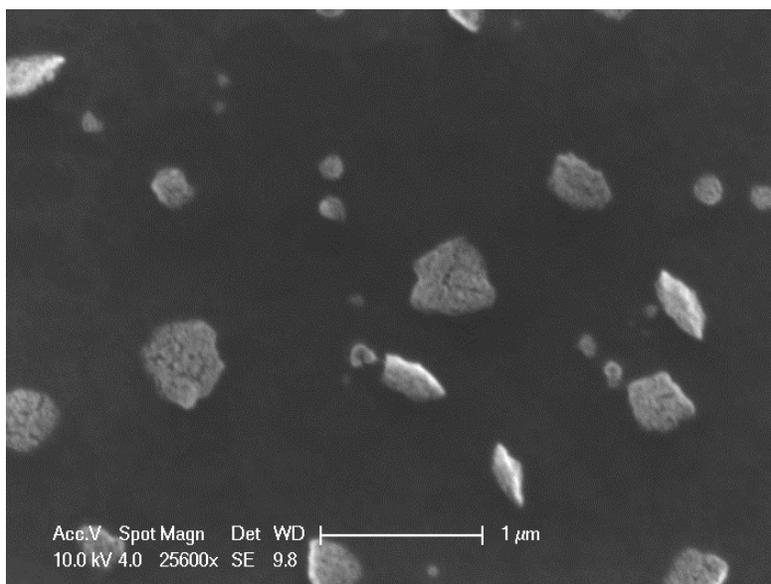

Fig S3. SEM characterization on larger Pt nanocluster

Table S1. Summarized properties of sputtered and solution deposited Pt layers on FTO: sheet resistance (R_s), Θ_c the contact angle measured between the Pt electrode and electrolyte after 30 sec and roughness of the Pt layers above FTO calculated by AFM.

Counter electrode layer	R_s^* (Ω/sq)	Θ_c (º)	Roughness$^\$$ (nm)
Spray-coated	22.3	22	7.56
Dip-coated	21.5	15	6
Brushed	23.4	21	8.44
Sputtered	19.6	15	5.92

$^*R_s$ have been calculated for a length of 5 mm.

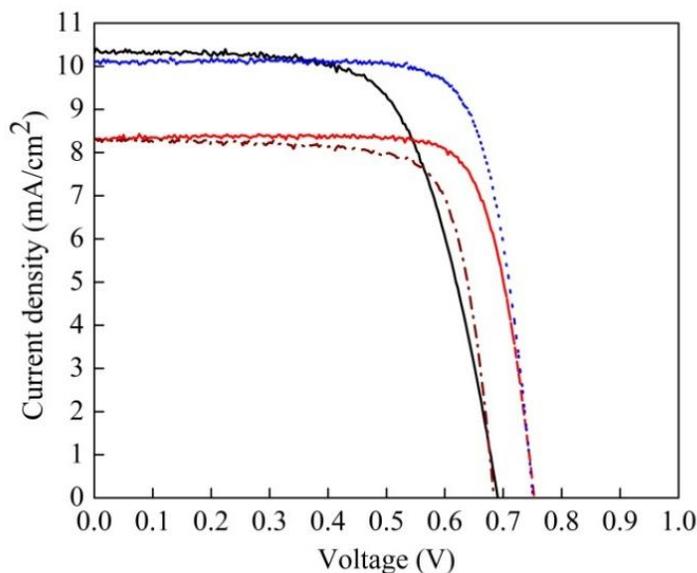$^\$$Arithmetic average of the absolute values measured by AFM.

Fig S4. Current −Voltage (I-V) measurement curves of N3 DSCs recorded under sunlight (~ 0.6 suns) of different deposited Pt-counter electrodes spray-coated (−), dip-coated (− −), brushed (¨) and sputtered (−·−).

The thickness of the sputtered Pt-counter electrode was increased to 40 nm by sputtering Pt for 150s at 30 mA at a distance of 3 cm. The N3 DSC device performances at 0.68 suns are V_{oc} (V) - 0.61, J_{sc} (mA/cm^2) - 7.99, Fill Factor (%) - 75%, Efficiency (%) - 5.35, R_s (Ω) - 33.7 and R_{sh} (Ω) - 19k. The results that were obtained with 40 nm sputtered Pt-counter electrode layer were decreased compared to other deposited Pt-counter electrodes. However, this type of Pt thickness dependent electrical performances on DSCs is reported in literature. [1, 2]

1. X. Fang, T. Ma, G. Guan, M. Akiyama, T. Kida, E. Abe, Journal of Electroanalytical Chemistry 570 (2004) 257-263.
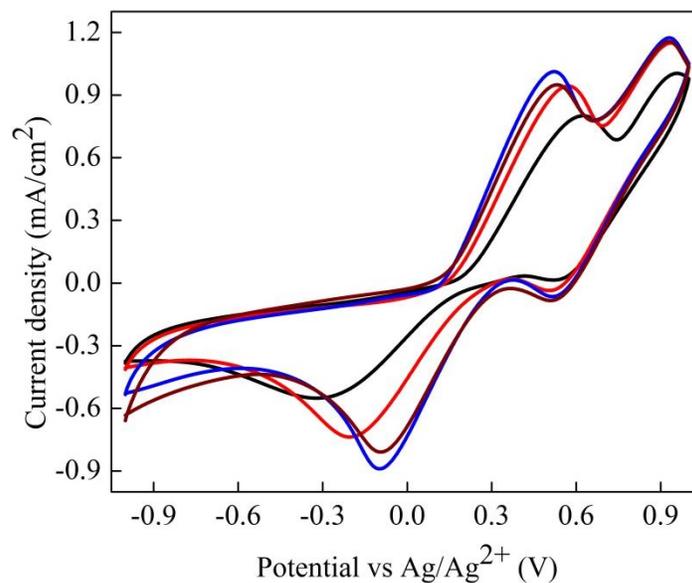2. A. Hauch, A. Georg, Electrochimica Acta 46 (2001) 3457-3466.

Fig S5. Cyclic voltammogram curves of different deposited Pt-counter electrodes spray-coated (black), dip-coated (red), brushed (blue) and sputtered (wine).

Electrochemical impedance spectra of N3 DSCs with different depositions of Pt-counter electrodes measured at 0.68 sunlight intensity are shown in Fig S6. The equivalent circuit used to fit these impedance spectra is shown in inset. The obtained Nyquist plots were fitted using ZSim software. The assessed values of the charge transfer resistances at the counter and working electrodes, the constant phase elements (CPE) at the interfaces of counter and working electrodes are presented in Table S2.
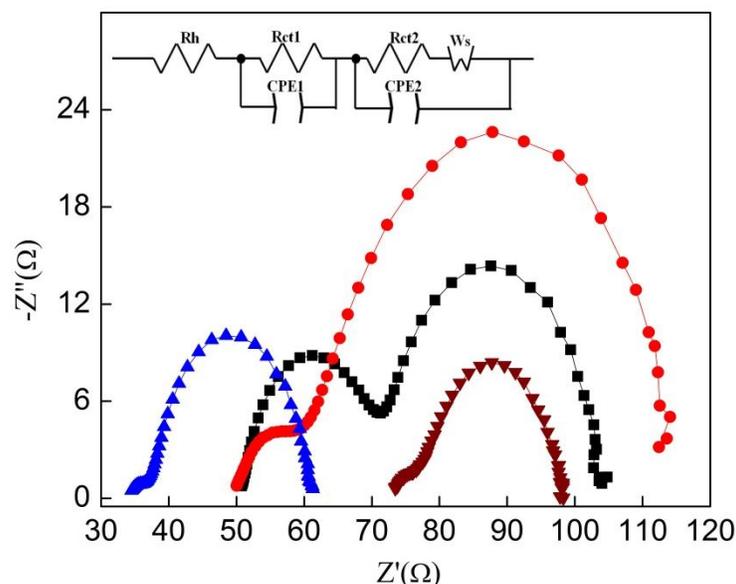
Fig S6. Nyquist plots of N3 DSCs with different counter electrodes of spray-coated (black), dip-coated (red), brushed (blue) and sputtered (wine) layers measured at 0.68 sunlight intensity. Inset shows the equivalent circuit diagram used to fit the impedance spectra. R_h: ohmic serial resistance; R_{ct1}: charge-transfer resistance of the counter electrode; CPE1: constant phase element of the counter electrode; R_{ct2}: charge-transfer resistance of the working electrode; CPE2: constant phase element of the working electrode and W_s: Warburg impedance.

Table S2. Impedance parameters of the DSCs estimated from the impedance spectra.

Counter electrode layer	R_h (Ω cm^2)	R_{ct1} (Ω cm^2)	CPE1 (F cm^{-2})	R_{ct2} (Ω cm^2)	CPE2 (F cm^{-2})	W_s
Spray-coated	10.64	4.059	2.7×10^{-5}	6.32	2.64×10^{-3}	2.26
Dip-coated	10.58	9.89	1.65×10^{-3}	2.23	4.69×10^{-5}	1.87
Brushed	7.26	0.58	1.8×10^{-3}	4.43	3.3×10^{-3}	2.96
Sputtered	15.31	0.9	1.04×10^{-3}	3.7	1.9×10^{-3}	3.68

The constant phase element (CPE) is parameter that dependents on frequency. This is engaged in the modelled circuit to estimate the capacitance resulted from the accumulation of ions at the electrode–electrolyte interface. For the rough electrodes, the CPE is more suitable than an ideal capacitor for simulating the AC response. Warburg impedance component is used in the modelled circuit to understand the diffusion phenomena. In the circuit first block consists of R_{ct1}/CPE1 representing the Pt-counter electrode-electrolyte and R_{ct2}/CPE2/W_s in the second block are allocated for the TiO$_2$/dye-electrolyte interfaces. The main study is to understand the catalytic action of the counter electrodes and this is governed by the parameter R_{ct1} (electron flow during the reduction of I$_3^-$ at the counter electrode). The R_{ct1}/CPE1 with respect to Pt-counter electrodes depends on the concentrations of the Pt solution used. This type of concentration dependent R_{ct1} of Pt layers behaviour has been observed elsewhere.[3] In this work,

for deposition of Pt-layers spray-coating was performed with the diluted Pt solution (concentration changed) two times, for dip-coating the concentration of Pt solution was same but dipping time was only for 1 min and for the formation of brushed Pt-layers we used 100 µl of Pt solution and completely dried in air. It can be clearly observed from AFM and SEM images larger nanoclusters were obtained from brushed technique than spray-coated and dip-coated techniques. The formation of these clusters could depend on the used concentration/dipping time of the Pt solutions. Due the change in the size of the Pt nanoclusters there is decrease of R_{ct1} with the increase in concentration of Pt solutions. The decrease of R_{ct1} accelerates the electrolyte reduction due to the larger active area of Pt nanoclusters. The smaller R_{ct1} increases the i_{ex} according to Buttler-Volmer equation.[3] The CPE also confirms that the larger active surface areas of the Pt-counter electrodes become larger with increase in size of Pt nanoclusters.

3. V.-D. Dao, C.Q. Tran, S.-H. Ko, H.-S. Choi, Journal of Materials Chemistry A 1 (2013) 4436-4443.